Misan Journal of Engineering Sciences ISSN-E: 2957-4250
Vol. 2, No. 2, December 2023 ISSN: 2957-4242

Enhancing Seismic Performance of Multi-story Steel Buildings Using Inner Mega Braced Frames

Ayman Z. Abdulhameed*[1], Mazin A. Ahmed[1] and Abdulamir A. Karim[1]

Civil Engineering Department, College of Engineering, University of Basrah, Basra 61006, Iraq

**Corresponding author E-mail: engpg.ayman.zaki@uobasrah.edu.iq*

(Received 13 Oct 2023, Revised 8 Dec 2023, Accepted 8 Dec 2023)

Abstract: Earthquakes are wide-ranging vibrations resulting from the movement of tectonic plates, causing damage to buildings. In this study, a multi-story steel building is designed using the ETABS v16 software under vertical loads only. Subsequently, seismic performance was enhanced by employing five different Mega braced frames (MBFs) systems in two cases: in the first case, the five bracing systems are placed within a frame located 6 meters away from the outer frame, while in the second case; the bracing systems were placed within a frame located 12 meters away from the outer frame. The building was then analyzed using nonlinear time history analysis with SAP 2000 V20 software, utilizing seismic data from the El-Centro earthquake available in SAP 2000 V20. The results were compared based on various parameters such as maximum roof displacement, maximum inter-story drift ratio, and maximum base shear. The findings demonstrated an improvement in the building's response, in the first case maximum roof displacement reduction ranging from 36.08% to 48.29% in both directions, and from 36% to 44% for maximum roof displacement in the second case. Maximum inter story- drift ratio also reduced by percentages ranging from 25% to 46% in the first case and 25% to 39% in the second case. From the analysis results, it is evident that the best pattern in the first case is pattern5, while in the second case pattern4 is the best.

Keywords: Non-linear time history analysis, seismic, Mega braced frames (MBFs), roof displacement

1. Introduction

As the utilization of tall steel braced structures has risen, there has been a growing emphasis on exploring different bracing configurations to achieve optimal performance while minimizing material usage. Bracing within the frames can either be confined to a single bay or extend across the entire facade of a structure. An early instance of single bay bracing used to resist lateral loads can be observed in the Empire State Building. One of the most renowned examples of extensive bracing on a large scale is the John Hancock Center in Chicago [1]. however External bracing on a larger scale, spanning multiple stories and bays, has been employed to create structures that are both highly efficient and visually appealing [2]. The diagonal elements spanning a bay or the façade of a building serve to unify the entire structure, essentially converting the building into a vertical cantilever beam. These diagonal braces can be likened to the webs typically found in truss structures, while the columns function as the chords of the truss, bearing substantial axial loads [2]. When comparing X-bracing and mega X-bracing, also known as diagrids, it was observed that diagrids exhibited a significant reduction in lateral drift, approximately 50% less, and resulted in a 25% reduction in material usage compared to traditional steel bracing [3]. Moreover, diagrid structures offer multiple advantages over alternative bracing systems. They enhance torsion resistance by effectively reducing shear deformation through diagonal braces. Moreover, diagrid structures provide greater structural flexibility, enabling the adjustment of module configurations and diagonal angles to optimize overall structural performance [4]. Several studies examining the seismic performance of bracing systems in tall buildings have been conducted previously; Di Sarno and Elnashai [5] evaluates the seismic performance of steel moment resisting frames (MRFs) enhanced with different bracing systems: special

concentrically braced frames (SCBFs), buckling-restrained braces (BRBFs), and mega-braces (MBFs). Through inelastic time-history analyses, MBFs were found to be the most cost-effective retrofitting option, resulting in a 70% average reduction in inter-story drifts, lower construction costs, and minimal business interruption during installation. Ghowsi and Sahoo 2015[6] In their study, the researchers examined the performance of chevron and split-X bracing systems when subjected to near-fault ground motions. Their findings led to the conclusion that the chevron bracing system exhibited greater stiffness and displayed brittle behavior. Lai and Mahin 2014 [7] Conducted an experimental and analytical investigation on bracing frames utilizing square hollow and round hollow sections. The findings indicated that the bracing frame incorporating round tubular sections demonstrated the ability to withstand larger story drifts compared to the specimen using square tubular sections.

The study aims to enhance the seismic performance of a multi-story steel structure of sixteen story using mega-braces in the inner frame with five different configurations of bracing systems. This is done in two cases: the first case involves placing the bracing systems at a distance of 6 meters from the outer frame, while the second scenario involves placing them at a distance of 12 meters from the outer frame. The comparison is then based on maximum roof displacement, maximum inter-story drift ratio, and maximum base shear while maintaining the same amount of steel in all models to determine the impact of the bracing system configuration on seismic performance improvement.

2. Case study

In this study, a steel building was designed using the ETABS V16 software [8], according to ASCE 7-16[9] for loads and ACI 318-14[10] for concrete solid deck slab while AISC 360-10 Code [11] is used to design steel sections (columns, beams, and secondary beams. The building consists of 16 floors, with the first floor having a height of 4 meters and the remaining floors having a height of 3.2 meters. Dead and live loads are described in table 1. It is divided into seven bays in X-direction and five bays in Y-direction as describe in Fig. 1, with the column arrange in the pattern each four story have the same section. The locations and the types of columns, beam and secondary beam are described in table 2.

Table 1 loads on the concrete solid deck slab [9]

No. of floors	Live load ($\frac{kN}{m^2}$)	Super dead loads ($\frac{kN}{m^2}$)
1st	5	3
2nd-16th	4	3

Table 2 locations of the columns and beams in the building.

No. of floor	column	External beam	Internal beam	Secondary beam
1-4	W14x176	W18x35	W16x45	W12x19
4-8	W14x120			
8-12	W14X90			
12-16	W14x61			

The specifications for the steel used in columns, beams and secondary beam are detailed in Table 3, and the steel used in the bracing systems is outlined in Table 4. Following the design process, performance improvement will be achieved by employing five distinct Mega Braced Frames (MBFs) within the interior frames. This enhancement will be examined in two cases. In the first case as described in Fig 2, the five bracing systems will be positioned within the frame situated 6 meters away from the perimeter frame in both X and Y directions. In the second case as described in Fig 3, the five bracing systems will be placed within the frame located at a distance of 12 meters from the perimeter frame in both directions. The analysis of these five bracing systems will be conducted using SAP 2000 V20 software, employing nonlinear time

history analysis and utilizing the El Centro earthquake data file. The comparison between the two Cases will be based on the following indicators: Maximum roof displacement, Maximum inter-storey Drift Ratio, and maximum base shear.

Table (3) Steel properties for beam, column and secondary beam.

Properties	symbols	value	unit
Unit weight	ρ_s	77	$\frac{kN}{m^3}$
Modulus of elasticity	E_s	200000	MPa
Poison's ratio	υ	0.3	-
Coefficient of thermal expansion	----	0.0000117	-
Shear modulus	G	76903	MPa
Minimum yield stress	F_y	345	MPa
Minimum tensile strength	F_u	448	MPa
Effective yield strength	F_{ye}	379	MPa
Effective tensile strength	F_{ue}	493	MPa

Table 4 properties of steel material for bracing

Properties	Item	Value	units
Unit weight	ρ_s	77	$\frac{kN}{m^3}$
Modulus of elasticity	E_s	200000	MPa
Poison's ratio	υ	0.3	-
Coefficient of thermal expansion	----	0.0000117	-
Shear modulus	G	76903	MPa
Minimum yield stress	F_y	250	MPa
Minimum tensile strength	F_u	400	MPa
expected yield strength	F_{ye}	379	MPa
expected tensile strength	F_{ue}	493	MPa

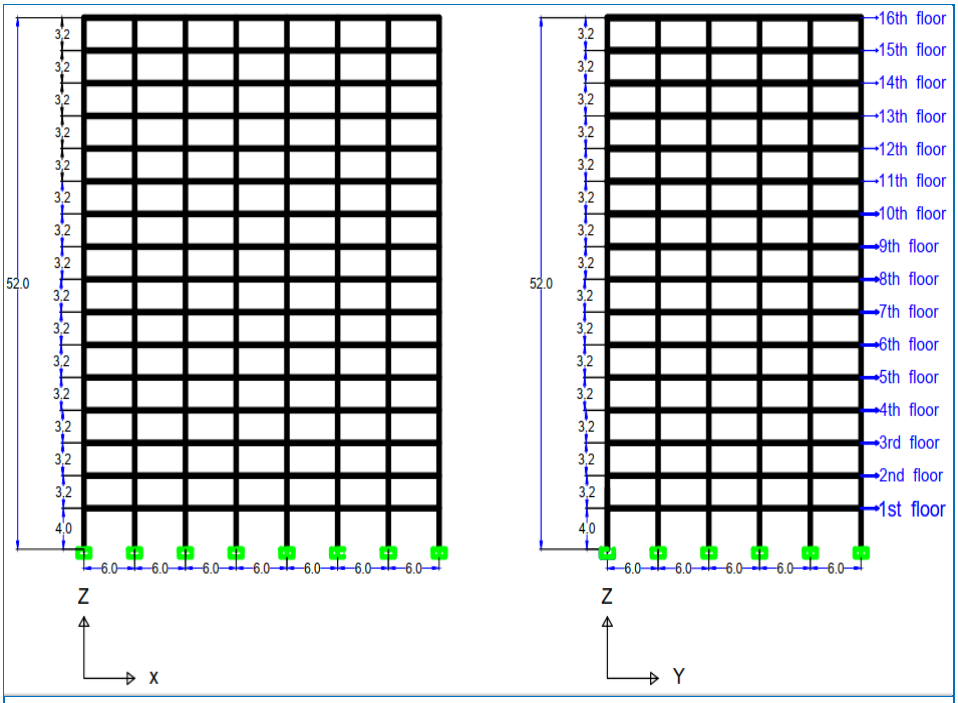

Fig. 1 X-Z and Y-Z Planes of the building.

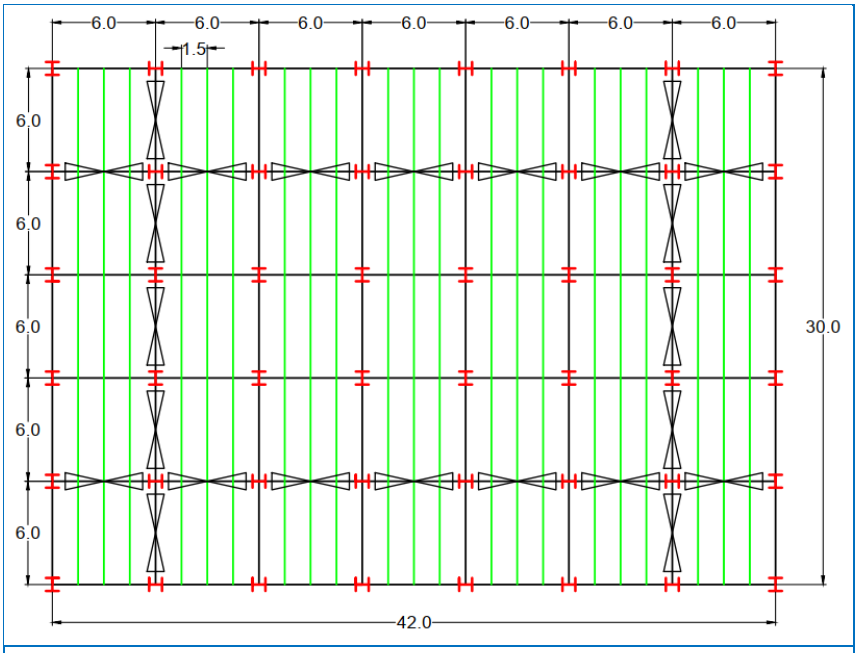

Fig. 2 plan view of case 1.

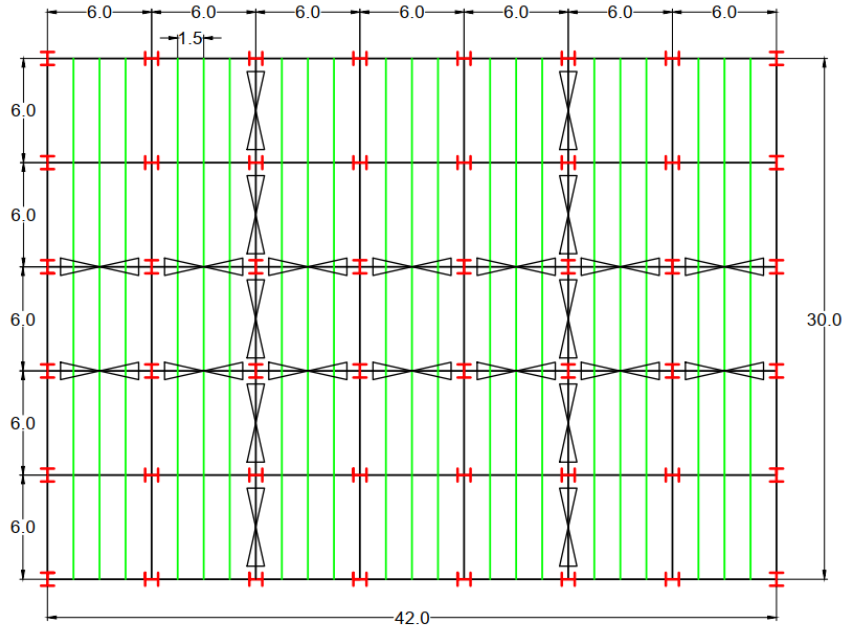

Fig. 3 plan view of case 2.

3. Bracing systems

3.1 Arrangement

In this study, the focus will be on finding the optimal location and arrangement of the bracing system that reduces and improves the performance of the building in terms of maximum roof displacement, maximum inter-story drift ratio, maximum base shear and maximum moment at the base of the building along the entire height of the building in both directions. It is ensured that the mass of bracing in each pattern is equal, satisfying architectural requirements to avoid obstructing the visibility of the building and limiting the number of bays where braces is placed on each face at every floor to a maximum of two braces. Various types of MBFs were used.

The mass of bracing is assumed constant at each story for all patterns and models. In the two cases, hollow structural section (HSS) bracing sections (circular pipe) were selected. It is further assumed that the bracing effectively resists earthquake loads in both tension and compression, aiming to simulate real-world conditions. The properties bracing material used are complying with ASTM A36 standard, with properties specified in Table 3.

The Patterns used in this research in two directions are:

1. Pattern1: building without bracing
2. Pattern2: Mega X-bracing.
3. Pattern3: Mega inverted V-bracing
4. Pattern4: Mega X-pattern with X-bracing in each Bayes
5. Pattern5: Mega X-bracing with diamond pattern.
6. Pattern6: Mega diamond pattern.

The explanation of the bracing sections utilized in the study can be found in Table 5, while Table 6 provides details on the weight and sections used for each model.

Table (5): sections and weight of braces

Bracing type	Floor	Sections (with each floor) (mm)	sectional Area (m^2)	Length (m)	Weight (kN) For each story
x-bracing (2 x- brace at each story face)	1-4	HSS 177.8x9.5	0.0047	6.8	19.68
	4-8	HSS 168.3x7.1	0.00335		14.03
	8-12	HSS 152x6.4	0.00272		11.39
	12-16	HSS127x4.8	0.0017		7.12
Double x-bracing (one x-brace in each story face)	1-4	HSS193X17	0.0094	6.8	19.68
	4-8	HSS179.4x12.8	0.0067		14.03
	8-12	HSS162.3x11.5	0.00544		11.39
	12-16	HSS134.6x8.59	0.0034		7.12
Inverted v-bracing (2 in each story face)	1-4	HSS186x13.4	0.0073	4.39	19.71
	4-8	HSS173.8x10	0.005146		13.90
	8-12	(HSS157.4x9.05)	0.004216		11.38
	12-16	(HSS130.9x6.75)	0.002633		7.11
Double inverted v-bracing (one at each story face)	1-4	(HSS209.3x25.2)	0.0146	4.39	19.71
	4-8	(HSS192x19.1)	0.0104		14.04
	8-12	(HSS173.6x17.2)	0.008451		11.41
	12-16	(HSS143.2x12.8)	0.005244		7.08

Table 6 the sections of bracing and weight of each model

No. of model	Floor numbers	sections	Weight (kN)	Total weight (kN)
1	-	-	-	-
2	1-4	HSS193X17	78.72	208.85
	4-8	HSS179.4x12.8	56.11	
	8-12	HSS162.3x11.5	45.56	
	12-16	HSS134.6x8.59	28.47	
3	1-3	HSS193X17	59.04	208.89
	4	HSS209.3x25.2	19.71	
	5-6-7	HSS179.4x12.8	42.08	
	8	HSS192x19.1	14.04	
	9-10-11	HSS162.3x11.5	34.17	
	12	HSS173.6x17.2	11.41	
	13-14-15	HSS134.6x8.59	21.36	
	16	HSS143.2x12.8	7.08	
4	1-3	HSS 177.8x9.5	59.04	208.86
	4	HSS193X17	19.68	
	5-6-7-8	HSS 168.3x7.1	56.11	
	9	HSS 152x6.4	11.39	
	10	HSS162.3x11.5	11.39	
	11-12	HSS 152x6.4	22.78	
	13-14-15	HSS127x4.8	21.36	
	16	HSS134.6x8.59	7.12	
5	1	HSS193X17	19.68	208.85
	2-3-4	HSS 177.8x9.5	59.04	
	5-6	HSS 168.3x7.1	28.05	
	7	HSS179.4x12.8	14.03	
	8	HSS 168.3x7.1	14.03	
	9-10-11-12	HSS 152x6.4	45.54	
	13	HSS134.6x8.59	7.12	
	14-15-16	HSS127x4.8	21.36	
6	1-2-3-4	HSS193X17	78.72	208.85
	5-6-7-8	HSS179.4x12.8	56.11	
	7-10-11-12	HSS162.3x11.5	45.56	
	13-14-15-16	HSS134.6x8.59	28.47	

3.2 Models (systems of arrangement of the bracing)

Pattern1: building without bracing

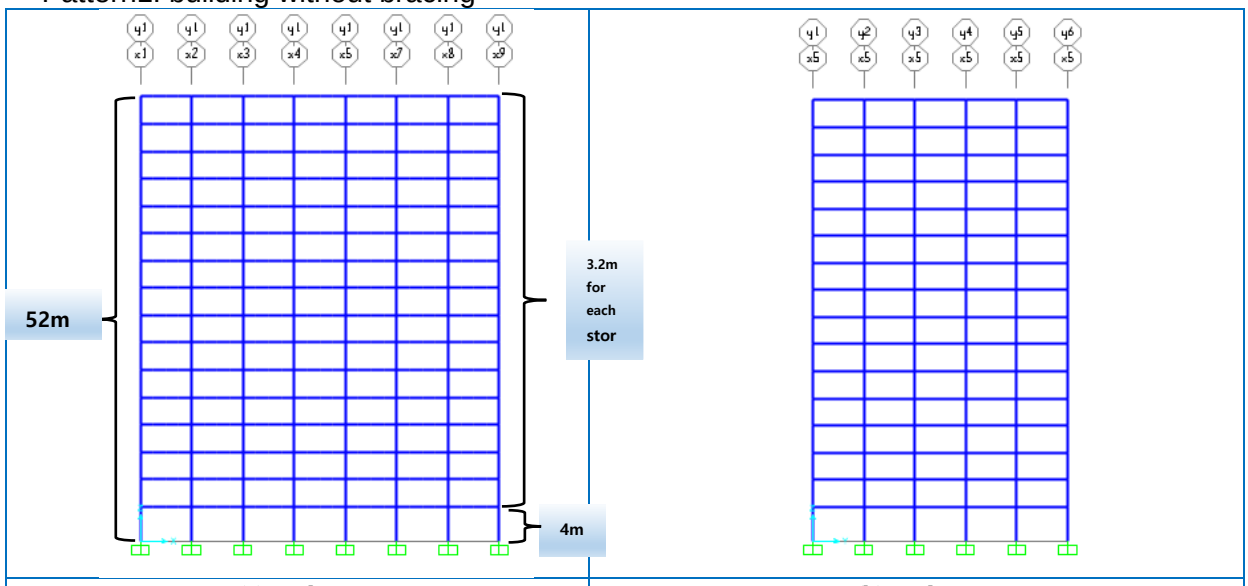

(a) X-direction (b) Y-direction

Fig. 4 Pattern1: building without bracing.

Pattern2: Mega X-bracing:

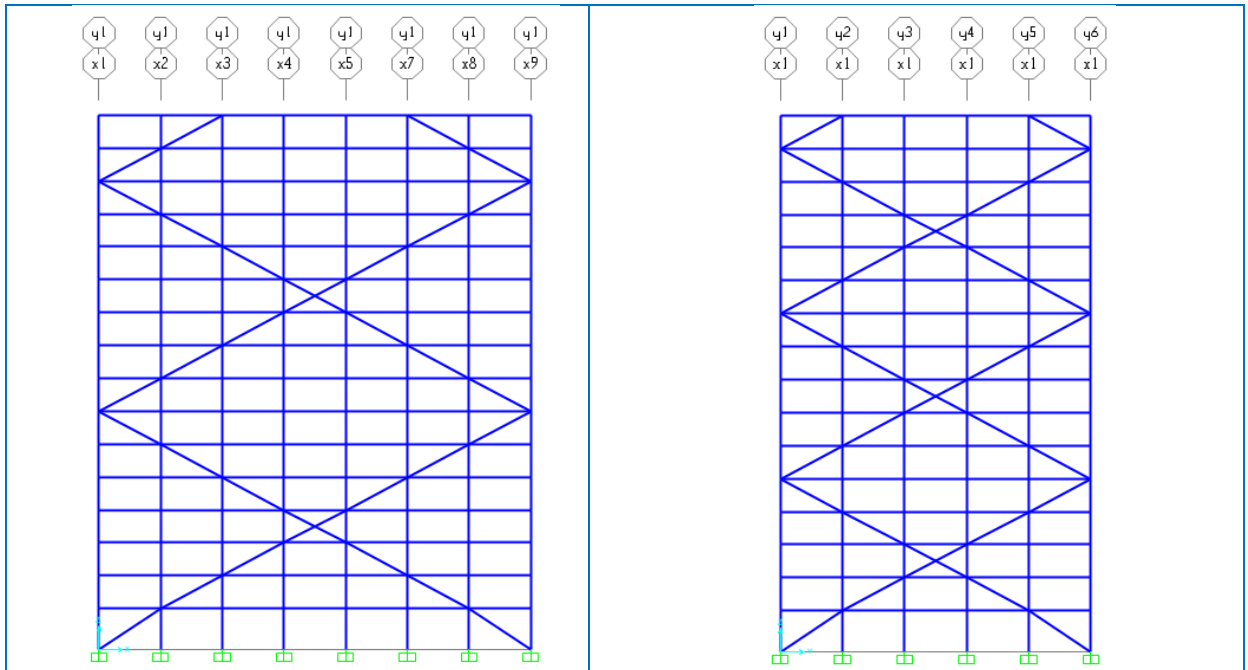

(a) X-direction (b) Y-direction

Fig. 5 Mega X-bracing.

Pattern3: Mega inverted V-bracing

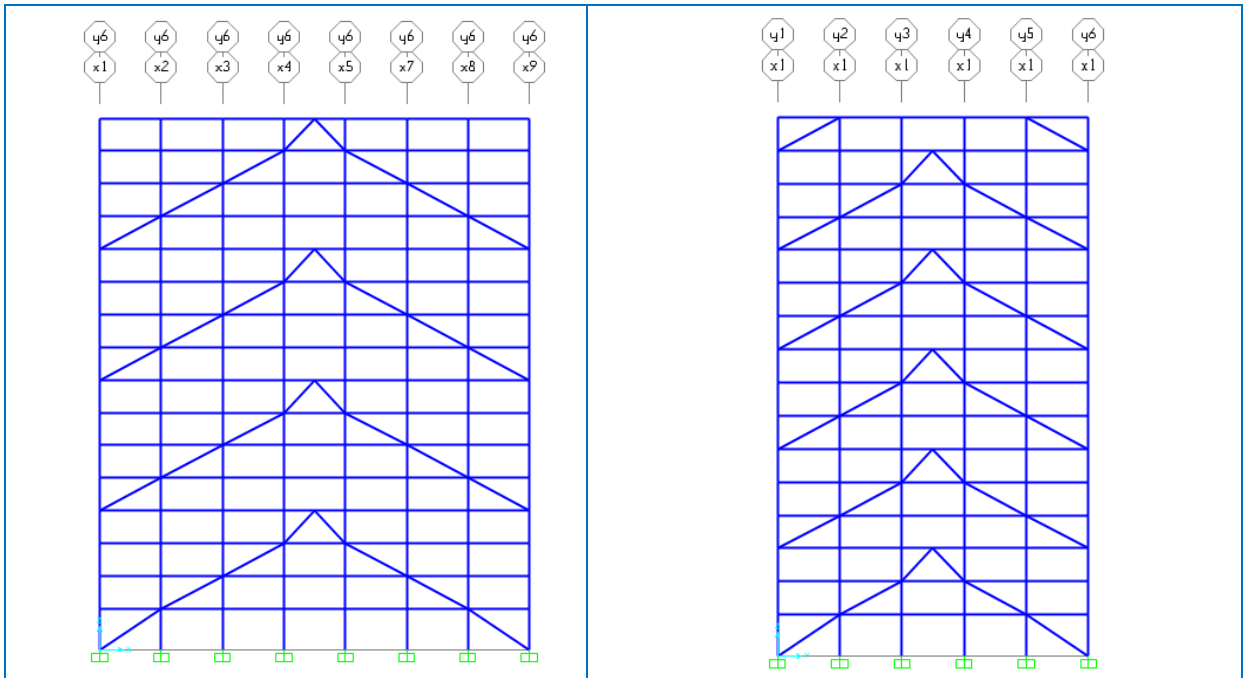

(a) X-direction (b) Y-direction

Fig. 6 Mega inverted V-bracing.

Pattern4: Mega x-pattern with X-bracing in each Bayes:

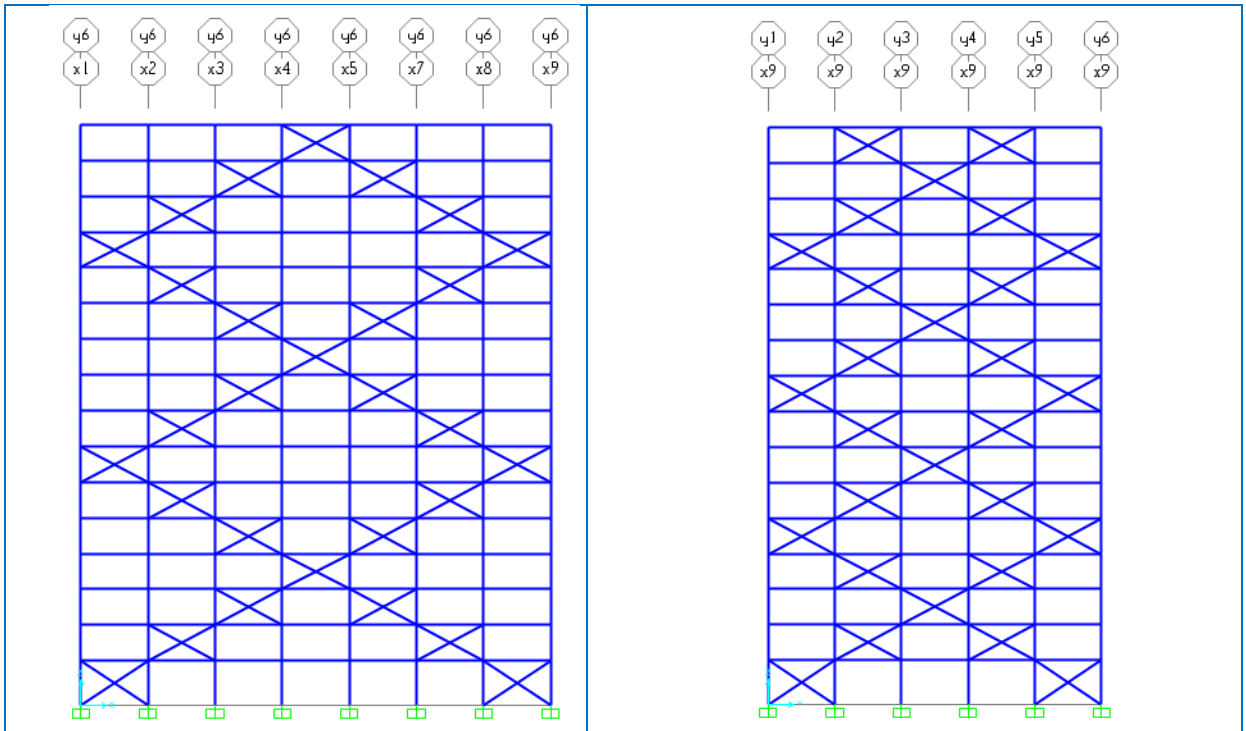

(a) X-direction (b) Y-direction

Fig. 7 Mega x-pattern with X-bracing in each Bayes.

Pattern5: Mega X-bracing with a diamond pattern:

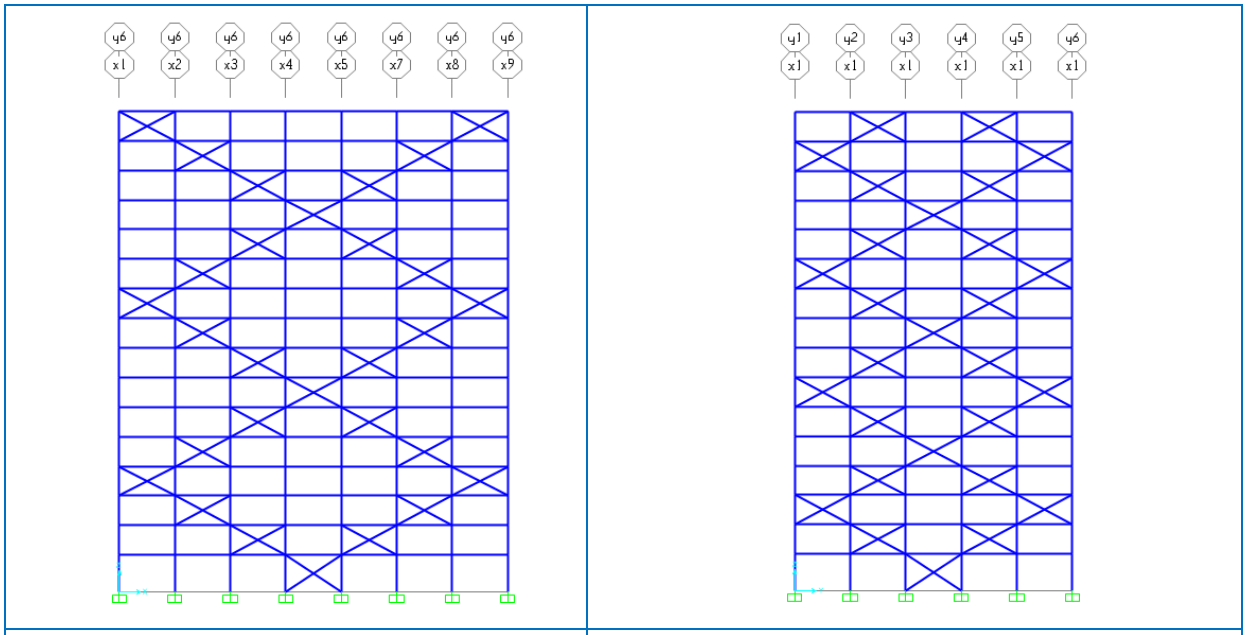

(a) X-direction (b) Y-direction

Fig. 7 Mega X-bracing with a diamond pattern.

Pattern6: Mega diamond pattern:

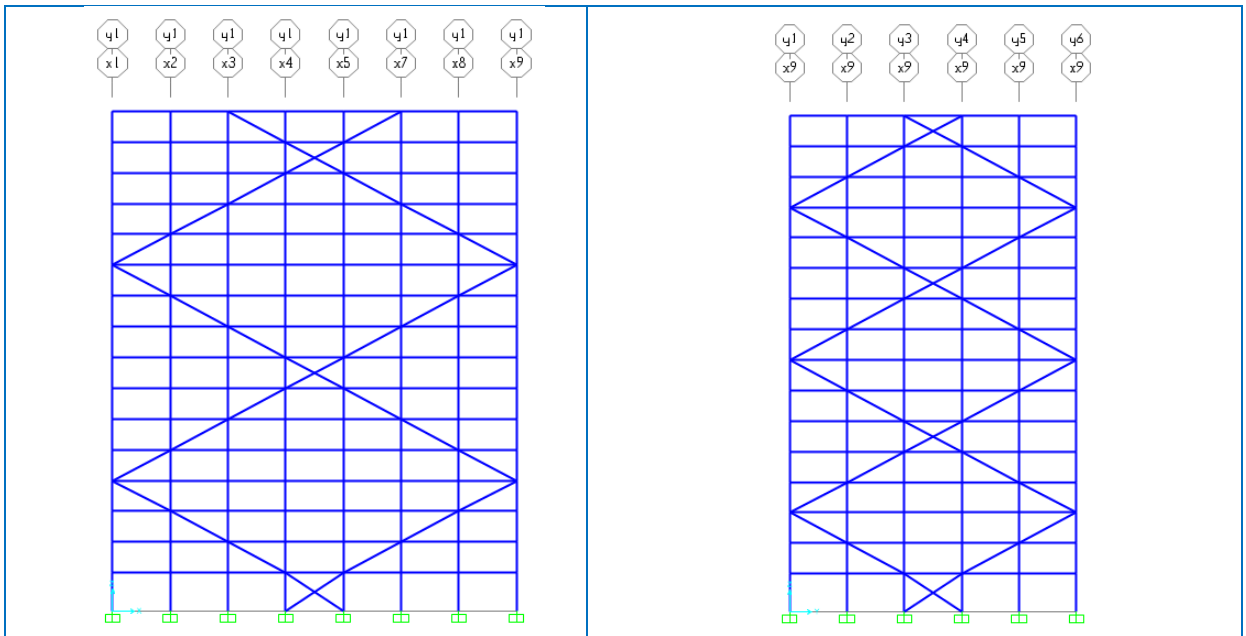

(a) X-direction (b) Y-direction

Fig. 8 Mega diamond pattern..

4. Analysis and results

Non-linear time history analysis by program sap2000 v20 was used to investigate the response of the steel structures under the El-Centro earthquake data and the function of El-Centro earthquake described in Fig.10 with duration 12.1 seconds and a time step of 0.02 second, with a damping ratio equal to 0.02 for steel structure [12].

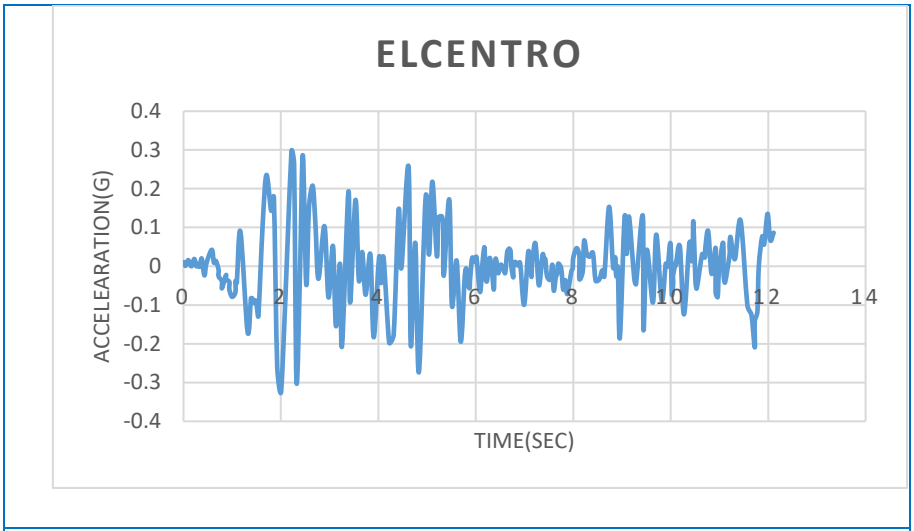

Fig. 10 El Centro earthquake, California in 1940 from SAP 2000 software data.

There are many parameters to compare between different models such as maximum roof displacement, maximum inter-story drift ratio, maximum base shear.

4.1. Maximum Roof Displacement

The analysis results in X-direction for the two cases as described in Fig. 11 and Fig. 12 show that in case 1 for Pattern2, Pattern3, Pattern4, Pattern5, and Pattern6, the maximum roof displacements are less than Pattern1which is without bracing by 41.37%, 42.39%, 44.52%, 48.29%, and 47.77%, respectively. On the other hand, in case 2 the roof displacement of Pattern2, Pattern3, Pattern4, Pattern5, and Pattern6, the roof displacements are less than that of Pattern1 by 41.2%, 42.3%, 44.2%, 42.7%, and 41.6%, respectively. In both Case 1 and Case 2, all models (Pattern2 through Pattern6) exhibit lower roof displacements in the x-direction compared to Pattern1. When compare between the two cases in X-direction it was found that the percentage reduction in roof displacement is generally higher in Case 1 compared to Case 2 for all models. Case 1 reductions range from approximately 41.37% to 48.29%, while Case 2 reductions range from approximately 41.2% to 44.2%. Pattern5 in Case 1 has the highest reduction in roof displacement (48.29%). Pattern4 in Case 2 has the highest reduction in roof displacement (44.2%).

In the Y-direction for case 1 maximum roof displacement for Pattern2, Pattern3, Pattern4, Pattern5, and Pattern6, are less than Pattern1(without bracing) by 36.08%, 38.81%, 41%, 44.34%, and 43.2%, respectively. While for case 2 maximum roof displacement for Pattern2, Pattern3, Pattern4, Pattern5, and Pattern6, the roof displacements are less than Pattern1 by 36.1%, 38.9%, 40.1%, 38.4%, and 38.3%, respectively. When compare for both cases (Case 1 and Case 2), all models (Pattern2, Pattern3, Pattern4, Pattern5, and Pattern6) exhibit lower maximum roof displacements in the Y-direction when compared to Pattern1 (without bracing). The reductions in maximum roof displacement vary slightly between the two cases but generally fall within the range of 36.08% to 44.34% for Case 1 and 36.1% to 40.1% for Case 2.

From the analysis, it is concluded the in case 1 pattern5 show the highest reduction in maximum roof displacement while for case 2 pattern4 show the highest reduction in maximum roof displacement, however the results in both cases showed that Pattern2, Pattern3, and Pattern4 exhibited nearly identical results in both the X and Y directions.

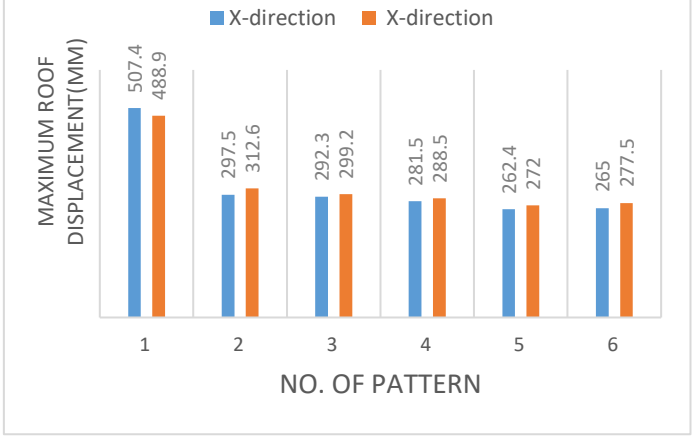

Fig. 11 maximum roof displacement (mm) for case 1

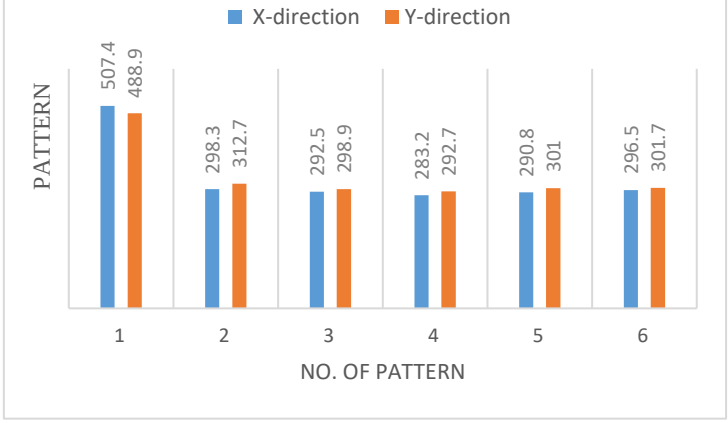

Fig. 12 maximum roof displacement (mm) for case 2

4.2 Maximum inter-story drift ratio

Inter-story drift ratio is determined by dividing the horizontal displacement between vertically aligned points at the upper and lower levels of a storey by the height of that storey. [9]

Non-linear time history analysis of the multistory steel building show that in X-direction for case 1 as describe in Fig 13 for Pattern2, Pattern3, Pattern4, Pattern5, and Pattern6, the maximum inter-storey drift decreased by 35.1%, 35.9%, 38.8%, 45.5%, and 43%, respectively. While for case 2 as describe in fig. 14 for Pattern2, Pattern3, Pattern4, Pattern5, and Pattern6, the maximum inter-storey drift decreased by 35.7%, 36.4%, 39.2%, 37.4%, and 34.9%, respectively.

As describe in fig. 15, In Y-direction for case 1 for Pattern2, Pattern3, Pattern4, Pattern5, and Pattern6, the maximum inter-storey drift decreases by 25.1%, 36.3%, 35.2%, 41.6%, and 38.2%, respectively. While for case 2 as describe in fig. 16 maximum inter-storey drift ratio for Pattern2, Pattern3, Pattern4, Pattern5, and Pattern6, the maximum inter-storey drift decreases by 25.4%, 36.4%, 35.4%, 33.5%, and 30.8%, respectively.

In case 1 pattern5 have the best performance in reducing maximum inter-story drift ratio in X and Y directions with respect to other models, otherwise in case 2 pattern4 have the best performance in reducing maximum inter-storey drift ratio with respect to other models.

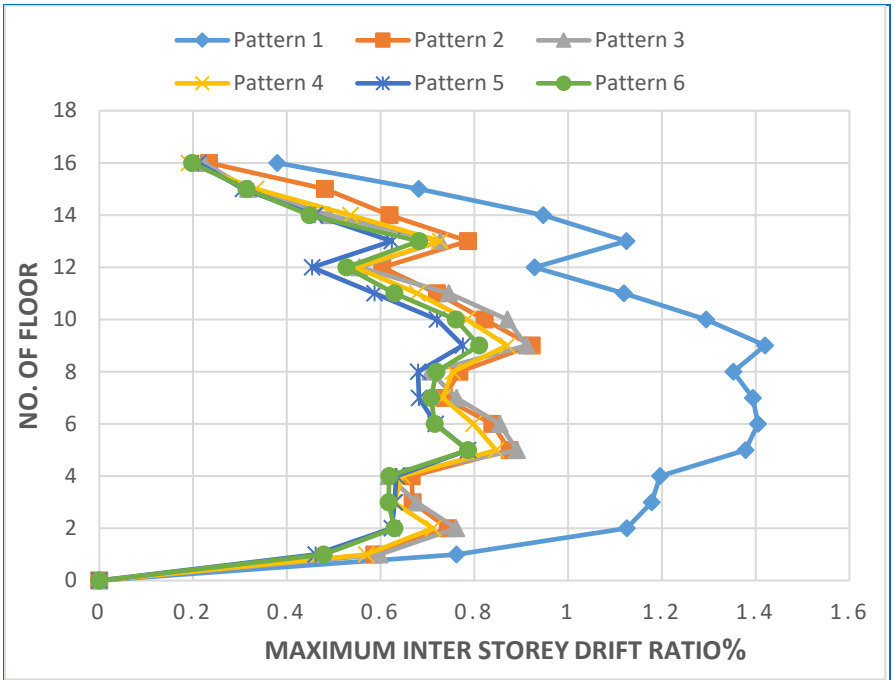

Fig. 13 maximum inter-story drift ratio case 1 (X-direction).

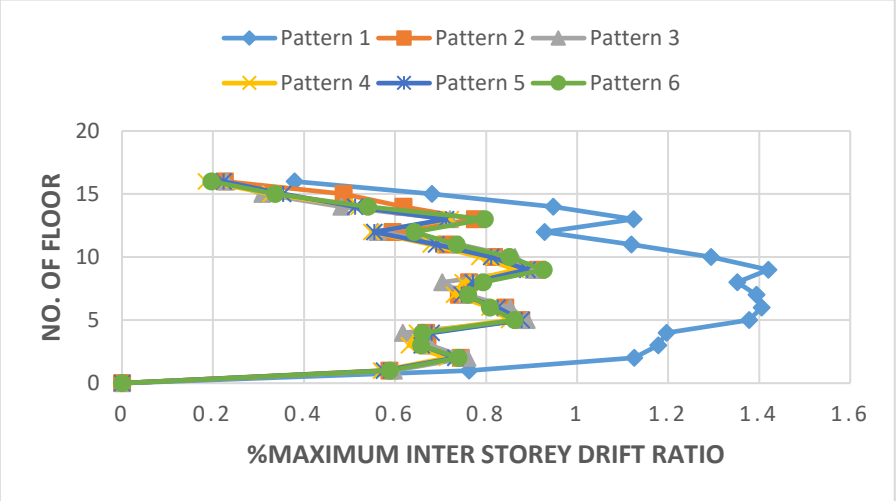

Fig. 14 maximum inter-story drift ratio case 2 (X-direction).

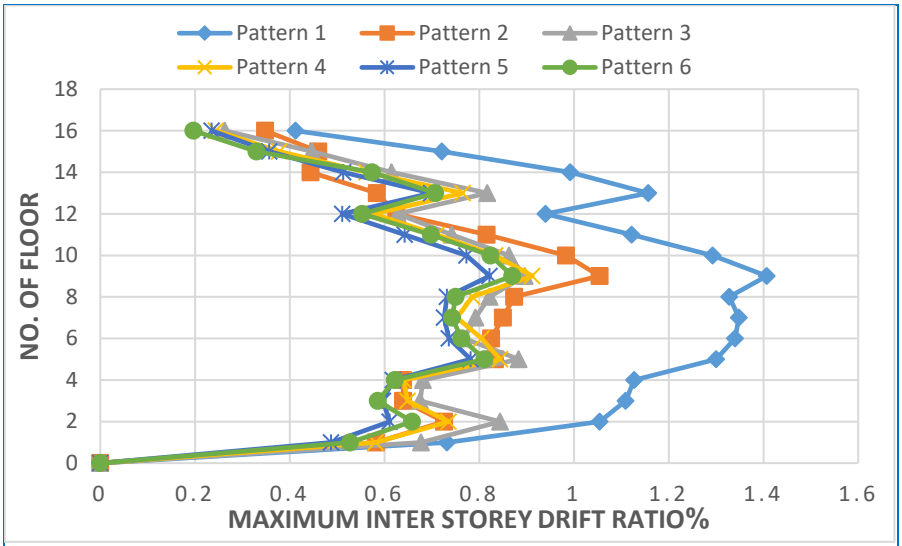

Fig. 15 maximum inter-story drift ratio case 1 (Y-direction).

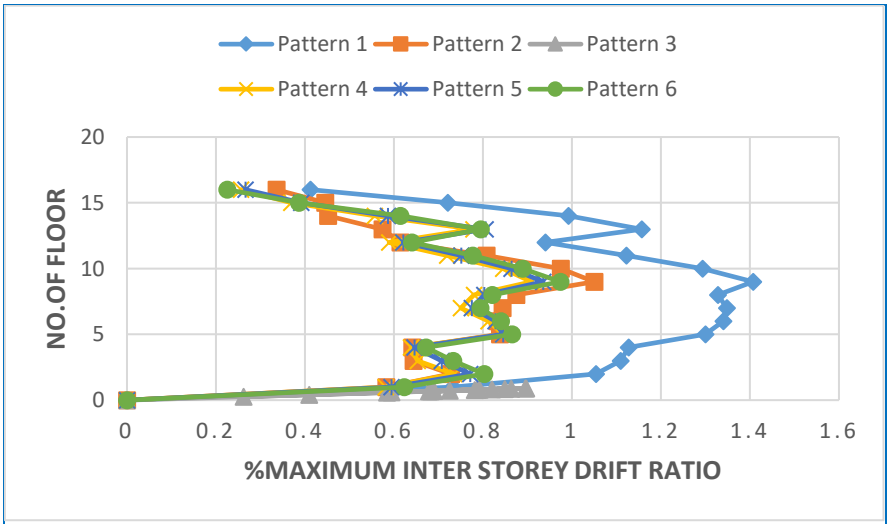

Fig. 16 maximum inter-story drift ratio case 2 (Y-direction).

4.3 Maximum Base Shear

It is the maximum lateral force occurs at the level where the horizontal seismic ground motion is assumed to be transferred to the structure [9].

When an earthquake occurs, the earthquake's acceleration is converted into a shearing force that influences the foundation of the structure. Through the application of principles related to Pseudo-acceleration, as described below, we can derive specific insights from the analysis [13].

$$V_{peak}=\frac{A}{g}*W \quad (1)$$

$$A=(\frac{2\pi}{T_n})^2*D \quad (2)$$

$$T_n=2\pi*\sqrt{\frac{m}{k}} \quad (3)$$

Where:

V_{peak}=peak base shear.

A=acceleration

W= Weight of the structure

g=gravitational acceleration

T_n=natural period of the structure

m=mass of the structure

K=stiffness of the structure

Introducing bracing into the structure reduces its natural period, thereby enhancing structural rigidity and stiffness as described by Formula (3). With a decrease in the natural period (Tn), the formula (2) indicates a corresponding rise in acceleration at the base of the structure, leading to an increased base shear as per Formula (1) compared to the scenario without bracing.

Non-linear time history analysis results as mentioned in table 7 and describe in Fig. 17 indicated that In Y-Direction for In Case 1, the maximum base shear (Fy) values for models 1 to 6 are 9454, 16248, 17538, 16017, 15027, and 15593 kN, respectively. While for Case 2, the maximum base shear (Fy) values for models 1 to 6 are 9454, 16276, 17659, 16057, 16276, and 16759 kN, respectively. From this results, it can be seen that in the Y-direction, the maximum base shear (Fy) values for Case 2 are generally slightly higher than those in Case 1 for most of the models. This indicates that, in general, Case 2 results in higher base shear in the Y-direction compared to Case 1.in other hand In X-Direction for Case 1, the maximum base shear (Fx) values for models 1 to 6 are 10134, 16381, 16538, 16002, 14782, and 15025 kN, respectively. While for Case 2, the maximum base shear (Fx) values for models 1 to 6 are 10134, 16420, 16548, 16033, 16197, and 16458 kN, respectively. In the X-direction, the maximum base shear (Fx) values for Case 2 are

also generally slightly higher than those in Case 1 for most of the models. This suggests that, like in the Y-direction, Case 2 results in higher base shear in the X-direction compared to Case 1.

The results of analysis show that in case 1, pattern5 have an increase in maximum base shear lower than models from pattern2 to pattern6 otherwise for case 2 pattern4 have an increase maximum base shear lower than other models.

In both the Y-direction and X-direction, Case 2 consistently produces slightly higher maximum base shear values compared to Case 1 for all six models. This indicates that Case 2 may result in higher lateral forces and stresses on the structure.

Table 7 maximum base shear for case 1 and case 2 in X and Y directions

No. of pattern	Case 1		Case 2	
	Y-direction	X-direction	Y-direction	X-direction
	Max. Fy (kN)	Max.Fx (kN)	Max. Fy (kN)	Max. Fx(kN)
1	9454	10134	9454	10134
2	16248	16381	16276	16420
3	17538	16538	17659	16548
4	16017	16002	16057	16033
5	15027	14782	16276	16197
6	15593	15025	16759	16458

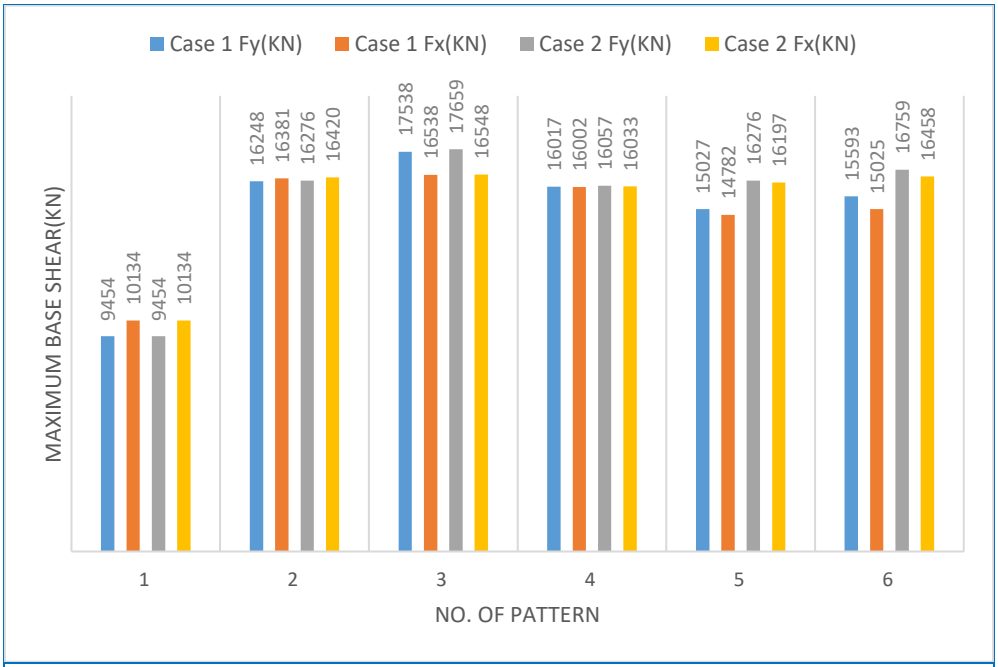

Fig. 17 maximum base shear for case 1 and case 2 in two directions

5. Summary and conclusions

From the non-linear time history, analysis results, the following conclusion may be drawn:

- Mega brace frames (MBFs) are highly effective in reducing maximum roof displacement in two different cases. In case 1, the reduction varies from 36.1% to 48.3% for both X and Y together, with pattern5 demonstrating the best performance among the models. In case 2, the reduction ranges from 36.1% to 44.2%, and pattern4 stands out as best choice among the available models.
- In both first and second cases, Pattern2, Pattern3, and Pattern4 exhibited nearly identical performance regarding maximum roof displacement in both directions.
- In Case 1, MBFs were found to reduce the maximum inter-story drift ratio by a percentage ranging from 25.1% to 45.5% in both directions. Pattern5 is identified as the most effective choice for improving performance. In Case 2, the reduction magnitude varies from 25.4% to 39.2% in both directions, with Pattern4 being the optimal selection. Furthermore, the analysis indicates that the reduction magnitude in the X-direction is greater than that in the Y-direction for both cases.
- When considering the maximum base shear, it is evident that the addition of a bracing system to a steel structure results in an increase in base shear for all patterns.
- Based on the analysis results, it is evident that the case 1 is slightly superior to the case 2 in all models and in both directions, as indicated by the maximum roof displacement, maximum floor drift, and maximum base shear.

References

[1] Taranath, B. S. (2016). *Structural analysis and design of tall buildings: Steel and composite construction*. CRC press.

[2] Smith, J., Coull, A., & Structures, T. B. (1991). *Analysis & Design*. Wiley and sons, New York.

[3] Yu, X., Ji, T., & Zheng, T. (2015). Relationships between internal forces, bracing patterns and lateral stiffnesses of a simple frame. *Engineering Structures, 89*, 147-161. http://dx.doi.org/10.1016/j.engstruct.2015.01.030

[4] Al-Kodmany, K., & Ali, M. M. (2016). An overview of structural and aesthetic developments in tall buildings using exterior bracing and diagrid systems. *International Journal of High-Rise Buildings, 5*(4), 271-291. http://dx.doi.org/10.21022/IJHRB.2016.5.4.271

[5] Di Sarno, L., & Elnashai, A. S. (2009). Bracing systems for seismic retrofitting of steel frames. *Journal of Constructional Steel Research*, *65*(2), 452-465. http://doi.org/10.1016/j.jcsr.2008.02.013

[6] Ghowsi, A. F., & Sahoo, D. R. (2015). Performance of medium-rise buckling-restrained braced frame under near field earthquakes. In *Advances in Structural Engineering: Dynamics, Volume Two* (pp. 841-854). Springer India. http://dx.doi.org/10.1007/978-81-322-2193-7_66

[7] Lai, J. W., & Mahin, S. A. (2014). Steel concentrically braced frames using tubular structural sections as bracing members: Design, full-scale testing and numerical simulation. *International Journal of Steel Structures*, *14*, 43-58. http://dx.doi.org/10.1007/s13296-014-1006-4

[8] CSI, C. (2015). Analysis reference manual for sap2000, etabs, safe and csibridge. *Computers and Structures, Inc., Berkeley, CA, USA*.

[9] American Society of Civil Engineers. (2017, June). Minimum design loads and associated criteria for buildings and other structures. American Society of Civil Engineers. http://doi.org/10.1061/9780784414248

[10] American Concrete Institute. (2014). ACI318, Building Code Requirements for Structural Concrete (ACI 318M-14) and Commentary (ACI 318RM-14).

[11] ansi, B. (2010)"AISC 360-10, specification for structural steel buildings." Chicago AISC.

[12] Chowdhury, I., & Dasgupta, S. P. (2009). *Dynamics of structure and foundation-a unified approach: 1 application*. CRC Press. http://dx.doi.org/10.1201/9781439832721

[13] Anil K. Chopra. (2014)"DYNAMICS OF STRUCTURES Theory and Applications to Earthquake Engineering". Prentice Hall.